AIAA JOURNAL
Vol. 30, No. 7, July 1992

High-Speed Propeller Noise Prediction—A Multidisciplinary Approach

Mark H. Dunn*
Lockheed Engineering & Sciences Company, Hampton Virginia 23666
and
F. Farassat†
NASA Langley Research Center, Hampton, Virginia 23665

The prediction of noise produced by advanced propellers is a multidisciplinary subject which involves the aeroelasticity, aerodynamics, and aeroacoustics of rotating blades. As part of the PTA (Propfan Test Assessment) noise-prediction project of NASA Langley, state-of-the-art computational methods in these disciplines were combined to form a comprehensive propeller noise-prediction package. The primary function of the project was to assess current noise-prediction capability. This was accomplished by comparing predictions with the extensive noise data provided by the PTA flight tests of NASA Lewis. The emphasis of this paper is on free-field predictions, which correspond to boom microphone measurements, and conditions for which the inflow is approximately axial. Predictions made on the fuselage of the PTA aircraft and predictions corresponding to nonaxial inflow conditions form the subject matter of companion papers by the authors and co-workers. Excellent agreement in trends and generally good agreement in acoustic levels between free-field measured and predicted data were observed. A secondary goal of a the project was to study systematically the effect of blade deformation on propeller aerodynamics and acoustics. The twist and camber distributions of advanced propellers are altered by centrifugal and aerodynamic forces. Consequently, blade surface pressure, power, and thrust are influenced by blade deformation. It was demonstrated that the impact of blade deformation on propeller noise can be significant and should be included.

Introduction

TWO desired characteristics of an aircraft propulsion system are high efficiency and low noise radiation. High propulsive efficiency results in low operating cost. Low noise radiation means community acceptance, passenger comfort, and lower aircraft empty weight due to the reduction of acoustic insulation in the fuselage. Thus, the noise issue also has economic impact on the sale and usage of aircraft.

A very attractive propulsor for high efficiency is the propeller. Modern advanced propellers have high disc loading and operate at supersonic helical tip speed. To reduce the radiated noise, the blades are thin and highly swept. Although high propulsive efficiency compared to current turbofans is achieved, the noise issue needs further attention. The current advanced turboprops generate high-intensity noise which must be reduced before these propulsion systems are considered for use in future airliners. Therefore, an important aspect of advanced propeller design is noise prediction.

In the last two decades, significant advances have been made in rotating blade noise prediction. It can be argued that the noise-generation mechanisms of advanced propellers are fully understood. Sophisticated codes based on the acoustic analogy are available for advanced propeller noise prediction which model the blade geometry and kinematics accurately. These codes require as input the deflected blade coordinates, surface pressure, and the flow in the blade vicinity (if quadrupole noise calculations are performed). These input data should be provided from aeroelastic and aerodynamic codes. This indicates the multidisciplinary nature of propeller noise prediction. In the past, various groups of researchers have developed propeller aeroelastic and aerodynamic codes for blade flutter and integrity analysis and calculation of propeller power, thrust, and efficiency. These codes could certainly be used for supplying input data to a noise-prediction code. The main difficulties in doing so are that 1) the codes are not compatible and, because the volume of data transmitted between codes is enormous, interfaces among codes must be developed for automatic computer execution; and 2) since some of these codes require considerable computational time, a scheme should be devised that reduces computer execution time while maintaining a reasonable degree of accuracy.

In 1988, a full-scale advanced propeller was extensively tested under the Propfan Test Assessment (PTA) program by Lockheed Georgia. These tests covered a large range of operating conditions at various altitudes. Both external and cabin acoustic data were collected, as well as engine and propeller operating parameters. The availability of these data provided an opportunity to evaluate the state-of-the-art of advanced propeller noise prediction. Such a study was conducted as part of the PTA noise-prediction project of NASA Langley, in which the necessary aeroelastic, aerodynamic, and acoustic codes were evaluated and linked by interfaces. A data management system was developed for the project so that inconsistencies in the measured PTA data could be easily discovered and eliminated from consideration. In addition, various display options, such as contour plots of noise intensity on the fuselage, are available from the data management system. The combined noise-prediction package, which includes the data management system, state-of-the-art engineering codes, interfaces, and an executive system, was completed in April 1990. Since that time, large-scale automated predictions and comparison with experimental data have been attempted.

Presented as Paper 90-3934 at the AIAA 13th Aeroacoustics Conference, Talahassee, FL, Oct. 22-24, 1990; received March 11, 1991; revision received Dec. 12, 1991; accepted for publication Dec 12, 1991.

*Principle Engineer. Member AIAA.
†Senior Research Scientist, Applied Acoustics Branch. Associate Fellow AIAA.

PTA Flight Test

The PTA flight tests were designed to evaluate the noise characteristics and structural integrity of a single rotor, full-scale advanced propeller.[1] This propeller is designed for cruise flight of Mach 0.8 at 10.7 km (35,000 ft) altitude. The following is a brief description of the test hardware, instrumentation, and procedure. Readers should consult the appropriate NASA Contractor Reports[1,2] for more details.

Advanced Propfan SR-7L

The advanced propeller, which was designed by Hamilton Standard, was of tractor type. It had eight thin, highly swept blades using NACA series 16 airfoils in the outboard region and series 65 circular arc airfoils in the inboard region of the blades, which had a 45-deg leading-edge sweep at the tip. Figure 1 shows this advanced propeller, known as the SR-7L propfan design, as installed on the aircraft. The diameter of the propeller was 2.74 m (9 ft) with the design disc power loading of 257 kW/m^2 (32 shp/ft^2). The blades were made of composite materials with a central aluminum spar.

PTA Aircraft

The testbed aircraft was a Gulfstream Aerospace GII business jet aircraft (Fig. 1). The propulsion system for the propfan was installed on the left wing. The power to the propeller was transmitted by a gearbox, and the direction of rotation of the propeller was clockwise viewed from a position ahead of the disc (i.e., rotating upward at the inboard side). The nacelle tilt angle could be changed from -3 to $+2$ deg (relative to the fuselage reference plane) to vary the inflow angle. In this paper, the results of nacelle tilt angle of -1 deg are utilized since this tilt angle corresponds most closely to uniform inflow conditions.

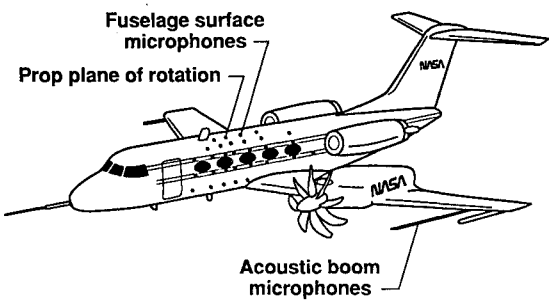

Fig. 1 PTA aircraft and the large-scale advanced propeller.

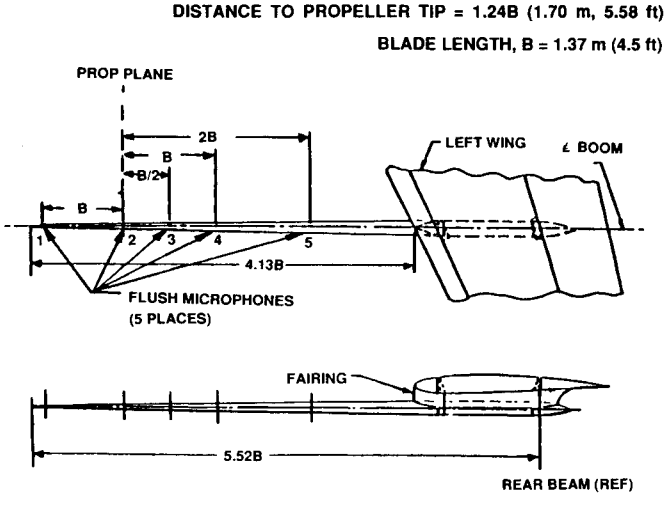

Fig. 2 Acoustic boom installation and microphone location.

Instrumentation

Extensive instrumentation was used in the PTA flight program. Some of the instrumentation was for the blade integrity evaluation.[1,2] For the purpose of this paper, only the external acoustic instrumentation will be covered here. On the exterior surface of the fuselage and on a wing-mounted boom, Kulite microphones of diameter 0.254 cm (0.1 in.) were mounted which had an accuracy of 1 dB from flight to flight. There were five microphones on the tapered boom. Figure 2 shows the boom design and the microphone positions. The boom is at the same distance from the propfan axis as the line nearest to the propfan axis on the fuselage. Since we will not present results for individual microphones on the fuselage, the microphone locations will not be given here. (See Table B-1 in Ref. 1 for more details.) Some important engine and flight conditions were measured during the tests by instruments carried onboard the aircraft. These were propfan rpm, blade pitch angle, engine torque, power and speed lever positions, sideslip angle, indicated air speed and Mach number, aircraft c.g. vertical acceleration, and the ambient air pressure and temperature.

Test Procedure

Both high-altitude and low-altitude flights were conducted with various nacelle tilt angles. In addition to acoustic objectives, the evaluation of propfan behavior under a wide range of dynamic loading conditions was of primary importance in the flight program. We are concerned with high-altitude tests in this paper. Three nacelle tilt angles of -3, -1, and 2 deg were used in these tests. A large range of flight parameter variations were tested. For each test, blade stress, noise, and vibration were recorded at each transducer point for approximately 60 s. The jet engine on the port side of the aircraft was operated at the lowest power setting needed for level flight. To evaluate the background noise, some tests were flown with propfan blades removed.

Data Acquisition

Acoustic data were recorded by FM recorders using the constant-bandwidth frequency division multiplexing technique. HP model 3562 narrowband analyzers were used for spectral analysis with 40 or 50 averages in the frequency range of 0–2000 Hz. The effective bandwidth of 3.75 Hz was achieved. For the most part, time histories of the acoustic signals are unavailable. With one exception, only spectral results are presented in this paper.

PTA Noise-Prediction Project

The PTA noise-prediction project was conducted at NASA Langley Research Center from January 1989 to December 1990 and was staffed by the authors and two co-workers. Details of the project objectives and its development are presented in this section.

Objectives

The primary objective of the PTA noise-prediction project was to evaluate the current status of noise-prediction technology for advanced technology propellers in actual flight. This was accomplished by the development of a system noise-prediction package that incorporates state-of-the-art methods in propeller aeroelasticity, aerodynamics, and aeroacoustics. The applicability of the prediction system was assessed by comparing predictions with actual flight data from the PTA tests, on both the acoustic boom and fuselage.

An advanced time domain propeller noise-prediction code, based on the acoustic analogy, provides the cornerstone for the system noise-prediction package. To be effective, the noise-prediction code requires accurate blade geometry and aerodynamic loading input. As a result, state-of-the-art propeller aeroelasticity and aerodynamics codes were identified and linked to the noise prediction code via software interfaces.

The scattering and refraction of incident acoustic waves by a hard surface such as a fuselage and its boundary layer are also important facets of system noise predition. Consequently, the noise-prediction package was augmented by the inclusion of a computer code that models these propagation effects. The final aspect of the development phase was the creation of an executive system that was designed to operate the codes and manipulate input and output data.

A secondary aim of the project was to study the effect of blade deformation on propeller aerodynamics and noise. In the past, because of the use of straight metal blades with low disc loading and relatively thick sections, blade deformation was not considered an important issue in aerodynamic and acoustic calculations. However, the new advanced propeller composite blades are highly loaded, thin, swept, and twisted. The blades can deform sufficiently to affect aerodynamics and noise. A systematic study of this effect has not been done before, and for this reason, was one of the objectives of this project.

Procedure

The comprehensive noise prediction package contains four major computer programs. Blade-deflection calculations are provided by the aeroelastic code NASTRAN.[3] The blade elastic behavior was supplied by a preprocessor known as COBSTRAN[4] which utilizes blade structural design and material properties to generate elasticity data to be used as input to NASTRAN. The output of COBSTRAN for SR-7L was obtained from NASA Lewis Research Center for use in this project. Blade surface pressures are supplied by Adamczyk's propeller aerodynamics code.[5] Free-field noise predictions are calculated by the propeller noise-prediction code ASSPIN,[6] and corrections due to the scattering and refraction of acoustical waves by a hard cylindrical surface (fuselage or boom) and its boundary layer are determined by the code MRS-BLP.[7] Brief descriptions of these codes are given in the next subsection, and the entire noise-prediction process is shown schematically in Fig. 3.

Blade deflection and blade surface aerodynamics are coupled phenomena. This is because precise deflected blade coordinates cannot be calculated without a knowledge of the aerodynamic loads and vice versa. Consequently, accurate blade coordinates and surface pressure data must be obtained by an iterative process between the aeroelasticity and aerodynamics codes. The iterative procedure is based on a similar process developed by August et al.[8] and proceeds as follows: The first iteration begins by executing NASTRAN without aerodynamic loads to get deformed (hot) blade coordinates due to centrifugal forces only. The second iteration cycle is now started by using the hot blade coordinates in the aerodynamic code. The aerodynamic code itself requires many iteration cycles for full convergence. Since at this stage, the hot blade coordinates are only approximate, the aerodynamic iteration cycles are stopped at a given cycle before full convergence. The resulting approximate blade loads are now used as input to NASTRAN, and new hot blade coordinates are computed which now have the effects of centrifugal forces and the approximate blade loads. This completes the second aeroelastic-aerodynamic iteration cycle. The third iteration cycle is then started by running the aerodynamic code with the latest hot blade coordinates but starting the aerodynamic iteration cycle with the approximate blade loads which were the result of the previous aerodynamic calculation. Again, the aerodynamic iteration cycles are stopped before full convergence. At this stage, the blade loads are more accurate than those computed in the second aeroelastic-aerodynamic iteration cycle. NASTRAN is then run with the latest aerodynamic loads, and the aerodynamic iteration is continued. Convergence between the two codes is attained when the blade angle at the 75% radial station does not change appreciably. This usually occurs after three complete iterations. For this reason, aerodynamic loads at each iteration of the interaction process are calculated using only one-third of the number of cycles normally needed for full convergence of the aerodynamics code. As a result, extraneous aerodynamic calculations are avoided and computational time is minimized.

When the aeroelastic-aerodynamic iterations have converged satisfactorily, the hot blade coordinates and blade surface pressures are used as input to the propeller noise code ASSPIN. This will give the free-field acoustics of the propeller. The results are compared with the measured acoustic data from the boom microphones after boom-scattering corrections are applied to the predictions. The boom-scattering corrections are calculated from MRS-BLP. To predict the propeller noise on the fuselage, ASSPIN is used to supply the incident pressure to MRS-BLP along the nearest line on the top of the boundary layer parallel to the propeller axis. MRS-BLP then gives the level of each harmonic of the noise on the fuselage surface.

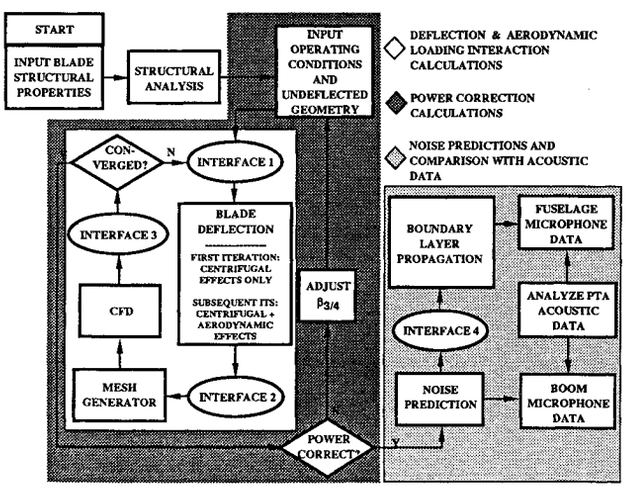

Fig. 3 PTA noise prediction procedure.

Code Descriptions

We present a brief description of the codes used in the prediction procedure. Readers are referred to the relevant references in this paper for more details.

NASTRAN

This code computes the blade deformation by centrifugal and aerodynamic forces.[3] The geometrically nonlinear (large displacement) analysis option of this code (NASTRAN SOL-64) is ordinarily used to obtain the aeroelastic computations reported here.[9] The NASTRAN input was supplied by the Composite Blade Structural Analyzer (COBSTRAN)[4] which computes the elastic characteristics of the blades based on the structural design and materials of blade construction.

Aerodynamic Codes

This code was developed by Adamcyzk and coworkers at NASA Lewis Research Center[10] and is based on the time-averaged Euler equation.[5] The flowfield is steady in time and periodic azimuthally in the rotating frame fixed to the propeller. The finite volume method of Jameson based on a Runge-Kutta scheme is utilized in this code. An iterative procedure is used to solve the average-passage equation system through the propeller. This code requires the propeller hub design for the blade load calculations.

ASSPIN

This code was developed by Dunn et al. at NASA Langley Research Center.[6,11] In this code, the subsonic source formulation 1-A[12] and transonic/supersonic source formulation 3[13] of

Farassat are used with automatic switching between the formulations in the code as needed. The formulations are based on the Ffowcs Williams-Hawkings (FW-H) equation without the quadrupole term. Thus, the acoustic formulations for noise generation are assumed to be linear. This appears to be a reasonable approximation because of the use of blades with very thin sections. The computational methods employed, the algorithm for coding, and sensitivity to time and surface mesh sizes of ASSPIN are reported in Refs. 6 and 11.

MRS-BLP

The theoretical formulation for the boundary-layer propagation code was derived by McAninch and Rawls,[14] and the code, known as MRS-BLP, for a cylindrical fuselage was developed by Spence.[7] The problem of wave propagation is solved in the frame fixed to the infinite cylinder with an incident wave prescribed on the top of the boundary layer from ASSPIN. The problem is solved in the frequency domain for each harmonic of the blade-passing frequency of the incident pressure. By using a Fourier transform in the axial direction, a single linear ordinary differential equation is obtained which is integrated numerically in the radial direction to find the acoustic pressure on the fuselage.[14] An incoming wave of unit amplitude is integrated outward from the fuselage surface to the top of the boundary layer, and the amplitude is matched to the incident pressure there by adjusting the wave amplitude. To save computation time, ASSPIN is only executed for observer positions along a line on the top of the boundary layer nearest to the propeller axis. The incident pressure along the top of the boundary layer around the remainder of the cylindrical surface is reconstructed by Graf's theorem for cylindrical (Hankel) functions.[15] A users manual for the code can be found in Ref. 7.

Results

In this section, results of the prediction effort corresponding to a nacelle tilt angle of -1 deg at the design cruise altitude of 10.7 km (35,000 ft) are presented. Measurements to validate uniformity of the inflow velocity were not taken during the PTA flight tests. Theoretical calculations performed by Lockheed, however, indicate that approximate uniform inflow conditions existed for many of the flight tests at the -1 deg tilt angle. Predictions for nacelle tilt angles other than -1 deg, corresponding to nonaxial inflow conditions, were a part of the project and can be found in Ref. 16.

Only the results for the acoustic boom are considered in this paper. Reports by other members of the PTA noise-prediction project team have been written in which fuselage predictions and comparisons with PTA data have been conducted. In Ref. 17, PTA measured data on the fuselage were processed and analyzed, and trends relating shaft horsepower, helical tip Mach numbers, and angle-of-attack effects to fuselage noise levels were established. By using the boundary-layer propagation code MRS-BLP, the effects of boundary-layer profile and thickness on fuselage noise were studied in Ref. 18.

The operating conditions chosen for the studies considered here represent a wide range of propfan horsepower and tip speeds and are shown in Table 1.

Aeroelastic-Aerodynamic Interaction Predictions

The effects of blade deflection on propfan aerodynamics and noise are discussed in this subsection. As shown in the prediction procedure (Fig. 3), the aeroelastic-aerodynamic iteration scheme also has a power loop in which the pitch angle at the 3/4 radial position, $\beta_{3/4}$, is adjusted so that the calculated power matches the measured power of the engine. All of the results presented in this subsection include the power loop calculations.

Results for the design condition (condition 264) are considered first. Figure 4 shows the results of several aeroelastic-aerodynamic iterations on the twist-angle distribution of a blade. Note that the curve labeled centrifugal loads is the result of the first aeroelastic-aerodynamic iteration in which the response due to the aerodynamic loads was not included. As expected, the outboard region of the blade is influenced most by the deflection. The maximum change in twist is about 4 deg (untwist) at the tip. As shown in Fig. 4, the aerodynamic loads produced only a small additional untwist. This curve is the result of the third and final aeroelastic-aerodynamic iteration illustrating the rapid convergence of this process.

Figures 5a and 5b show the deflection of the camber by centrifugal and aerodynamic loads at 81 and 100% radial positions, respectively. Note that the vertical coordinate in this figure is exaggerated. Several results are inferred from this figure. First, there is a change of up to 30% in maximum camber, and this deflection has opposite sense in the two radial positions. The camber is increased at the 81% location and decreased at the tip section. In both cases, the effect of the

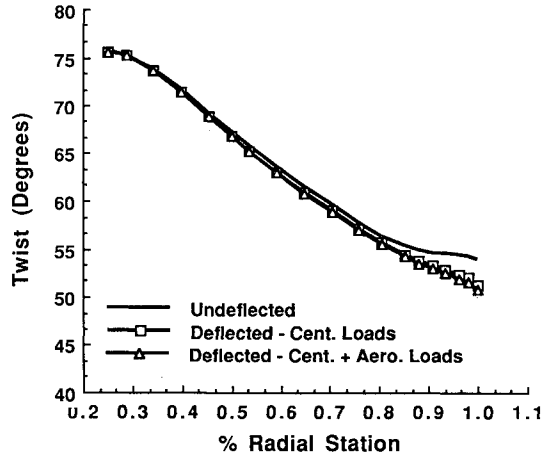

Fig. 4 Effects of centrifugal and aerodynamic loads on blade twist distribution-design condition (condition 264).

Table 1 Operating conditions of PTA aircraft used for predictions altitude = 10.7 km (35,000 ft)

Condition	c_0, m/s	ρ_0, kg/m^3	M_F	M_{tip}	rpm	J	C_p	shp	C_T	$\beta_{3/4}$, deg
264	299.3	0.372	0.814	0.814	1696	3.14	1.73	3029	0.40	57.7
276	299.3	0.370	0.811	0.853	1777	2.99	0.37	746	−0.02	51.3
348	301.1	0.370	0.808	0.757	1586	3.35	2.11	3006	0.47	60.3
356	301.0	0.368	0.806	0.845	1770	2.99	0.77	1527	0.12	52.9
357	301.2	0.369	0.802	0.847	1776	2.97	0.37	741	0.00	52.1
360	301.1	0.368	0.808	0.756	1584	3.35	1.01	1426	0.14	54.5
361	301.2	0.369	0.805	0.758	1589	3.34	0.47	668	0.00	54.1
377	302.4	0.367	0.799	0.628	1322	3.99	0.70	570	−0.04	55.4
378	302.4	0.366	0.797	0.626	1318	3.99	1.62	1308	0.20	58.0
380	303.5	0.364	0.804	0.624	1318	4.04	3.20	2583	0.41	62.6
383	299.8	0.369	0.808	0.842	1757	3.01	1.56	3089	0.37	54.3

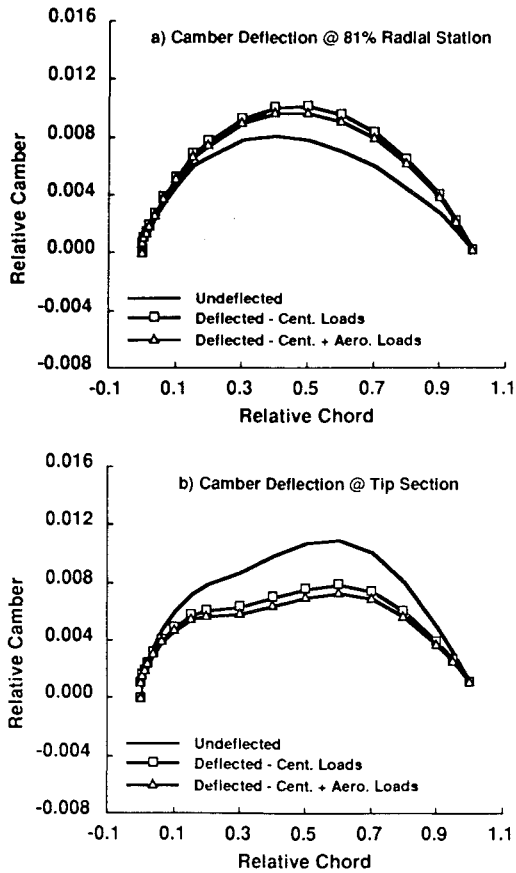

Fig. 5 Effect of centrifugal and aerodynamic loads on deformation of blade camber.

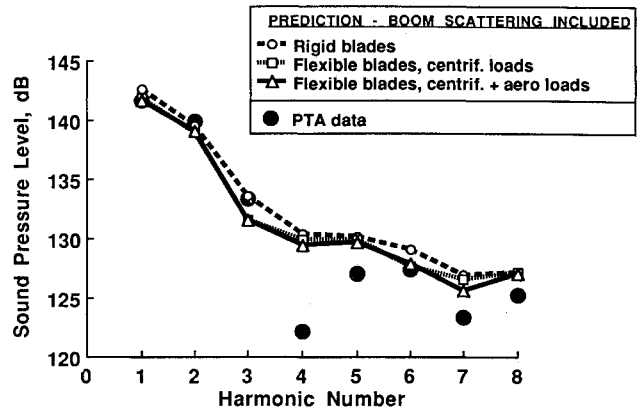

Fig. 6 Effect of blade deformation on the acoustic spectrum of boom microphone 3 [design condition (condition 264); power coefficient = 1.73 in all cases].

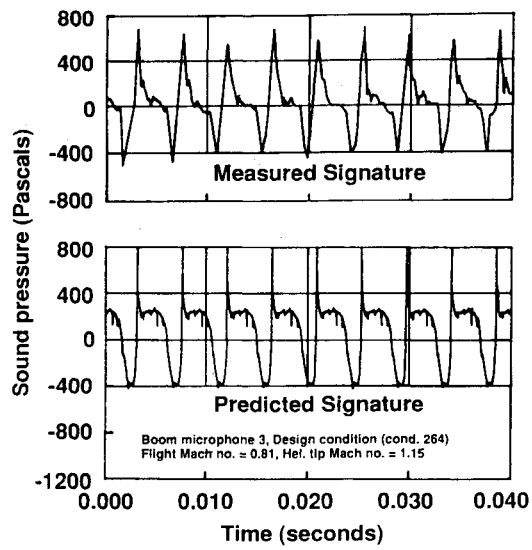

Fig. 7 Comparison of measured and predicted time histories for boom microphone 3 [design condition (condition 264)].

aerodynamic loading has been to reduce the camber. Also, it is seen that centrifugal forces account for most of the chordwise deflection. The smoothness of the deflected camber curves seems to indicate that the deflection calculations are stable.

Since the changes in blade twist and camber affect the aerodynamics, it is expected that there are differences in blade surface aerodynamic loads if cold and hot blade coordinates are used. Indeed, this is true. Using rigid (cold) blade coordinates, the predicted power coefficient for the design condition (condition 264) was 1.99 which was 15% higher than the measured power coefficient of 1.73. Note that to obtain the hot blade coordinates for use in the final aerodynamics calculations, airfoil thickness was added to the deflected camber shapes.

A summary of aeroelastic-aerodynamic calculations corresponding to the operating conditions of Table 1 is given in Table 2. Table 2 shows the measured and predicted thrust coefficient C_T, measured and predicted $\beta_{3/4}$, and predicted untwist angle at the tip. The thrust coefficients were not directly measured during the PTA flight tests, but were estimated from engine operating conditions. No assessment of the degree of accuracy of C_T measurements is available. The accuracy of $\beta_{3/4}$ measurements is estimated to be ± 1 deg (Ref. 2). From Table 2, it is seen that the untwist at the tip is between about 2–4 deg for all conditions. Thrust coefficients are consistently overpredicted, particularly for small values of C_T. A similar situation exists for $\beta_{3/4}$, although there is no consistency of behavior. Since the measurements of C_T and $\beta_{3/4}$ were

Table 2 Results of aeroelastic-aerodynamic calculations

Condition	rpm Measured	C_P Measured	C_T Measured	C_T Predicted	$\beta_{3/4}$, deg Measured	$\beta_{3/4}$, deg Predicted	$\Delta\beta_{tip}$, deg Predicted
264	1696	1.73	0.40	0.47	57.7	57.2	−3.3
276	1777	0.37	−0.02	0.07	51.3	50.9	−3.8
348	1586	2.11	0.47	0.58	60.3	60.2	−2.9
356	1770	0.77	0.12	0.23	52.9	52.5	−3.7
357	1776	0.37	0.00	0.13	52.1	51.0	−3.8
360	1584	1.01	0.14	0.27	54.5	55.2	−3.2
361	1589	0.47	0.00	0.10	54.1	53.1	−3.5
377	1322	0.70	−0.04	0.19	55.4	58.1	−2.1
378	1318	1.62	0.20	0.39	58.0	61.2	−2.2
380	1318	3.20	0.41	0.57	62.6	64.3	−1.9
383	1757	1.56	0.37	0.49	54.3	56.2	−3.6

not precise, the differences between measured and predicted quantities could be attributed to measurement errors.

The impact of the blade-deflection components, i.e., deflection due to centrifugal loads and deflection due to aerodynamic loads, on propeller noise is now considered. For this purpose, two examples, corresponding to conditions 264 and 276 of Table 1, are studied. All noise results discussed here are for boom microphone 3 (see Fig. 2). Differences in aerodynamic loading are minimized by using the appropriate measured power coefficients.

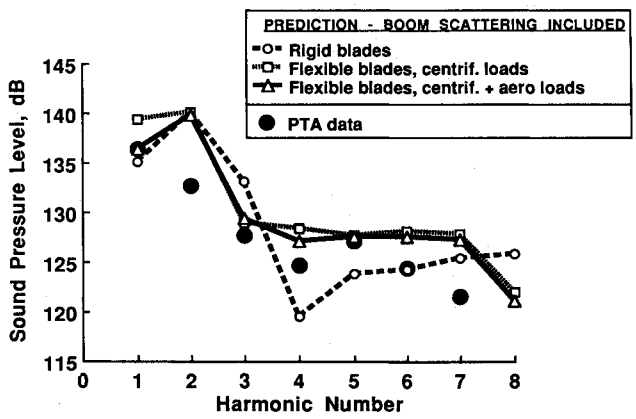

Fig. 8 Effect of blade deformation on the acoustic spectrum of boom microphone 3 [low aerodynamic loading condition (condition 276); power coefficient = 0.37 in all cases].

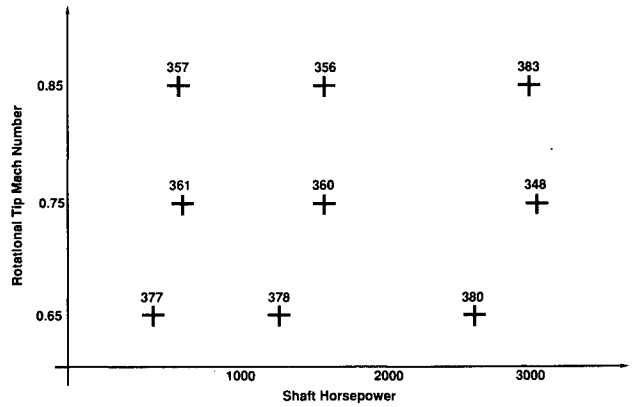

Fig. 9 Operating conditions for boom microphone directivity study (nominal flight Mach number = 0.8).

The condition 264 example is discussed first. Figure 6 presents the acoustic spectra using the rigid blade, blade deflected by centrifugal forces, and blade deflected by both centrifugal and blade forces. For comparison, the measured acoustic spectrum is also included. Note that a boom-scattering correction, calculated with MRS-BLP (see Ref. 19, Table 3), was added to the predicted spectra for the first three harmonics. For higher harmonics, a 6-dB correction was used. This figure shows that blade deflection, in this case, can produce as much as a 2-dB difference in some of the harmonic levels of the acoustic spectrum. In addition, the acoustic spectra of flexible blades with and without blade loads are very close. Comparison with the measured acoustic spectrum shows that, except for the third harmonic, the inclusion of blade deflection has improved the prediction. In Fig. 7, the measured and predicted acoustic pressure signatures are displayed. It is seen that the agreement is very good, both in peak values and shape of the signature. Note that no scattering correction is applied to the predicted signature.

Figure 8 shows the boom microphone 3 acoustic spectra for rigid and flexible blades for condition 276 (see Table 1). Again, a measured spectrum is included. For this condition, the propeller operates at low power coefficient relative to the previous example. This figure is shown to indicate that blade deformation can have a very significant influence on the level of some harmonics. For example, the fourth harmonic level for the rigid blade is about 10 dB lower than that of the flexible blade. The difference for most of the other harmonics is also significant. Another important point to note is that the inclusion of blade aerodynamic loads in the deformation calculation is important for the first harmonic level. For other harmonic levels, it does not appear to be significant. The inclusion of deformation, particularly by blade loads, in acoustic calculations have improved the prediction for all harmonic levels except the sixth and seventh.

Boom-Directivity Predictions

The results and discussions presented in this subsection concern the last nine conditions in Table 1. The flight Mach number of the aircraft was approximately 0.8 for each case in

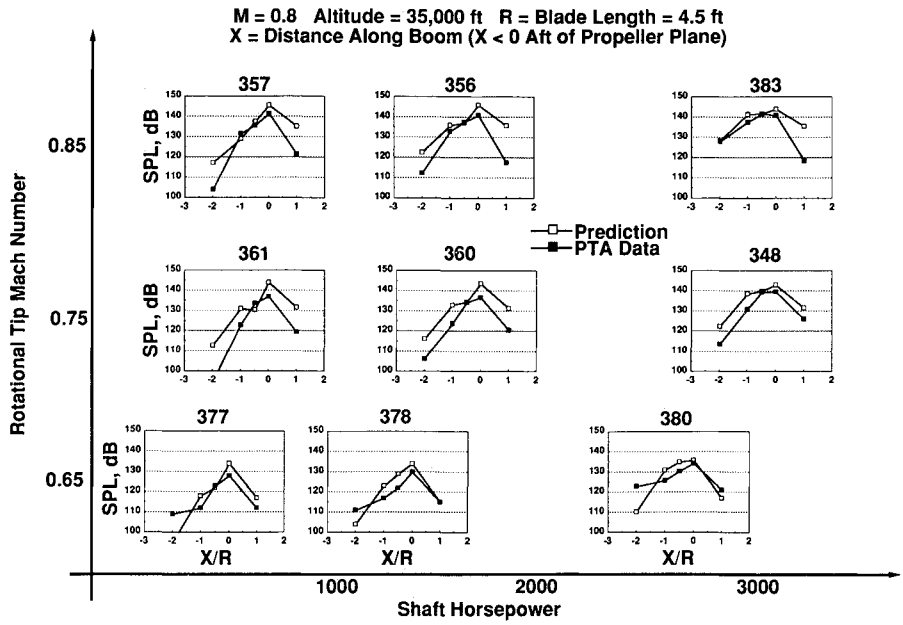

Fig. 10a Comparison of measured and predicted axial directivity for boom microphones corresponding to operating conditions of Fig. 9 (first harmonic).

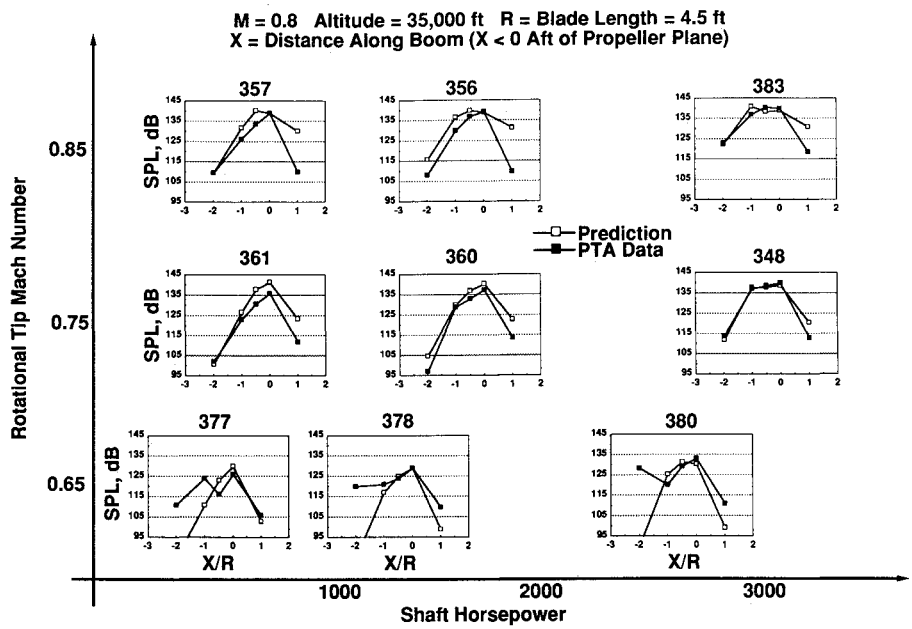

Fig. 10b Comparison of measured and predicted axial directivity for boom microphones corresponding to operating conditions of Fig. 9 (second harmonic).

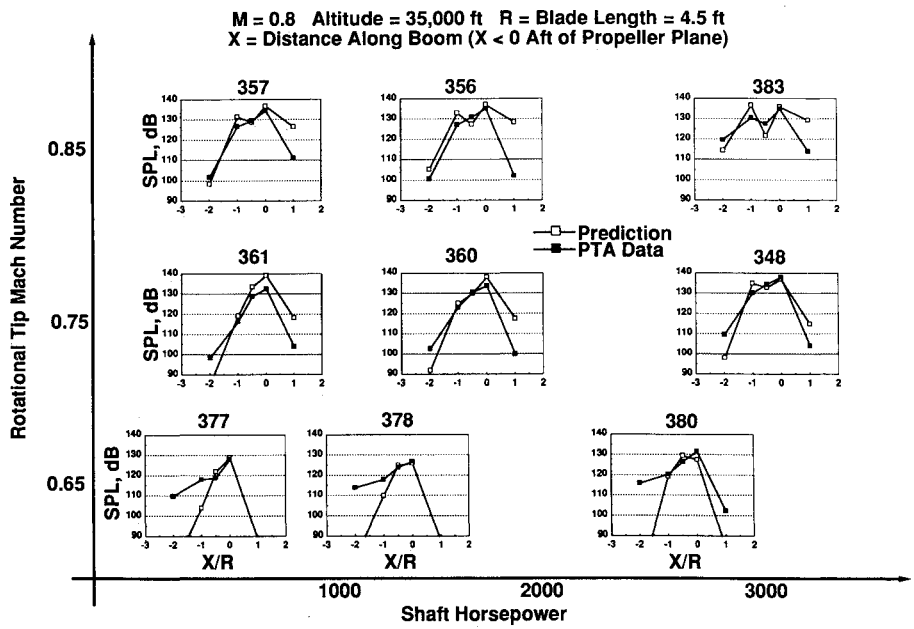

Fig. 10c Comparison of measured and predicted axial directivity for boom microphones corresponding to operating conditions of Fig. 9 (third harmonic).

Table 1. Furthermore, various rotational tip Mach numbers and shaft hosepower settings are represented. For a fixed-flight Mach number of 0.8, these operating conditions allow for a study of the effect of rotational tip Mach number and shaft horsepower on noise directivity along the acoustic boom, in which predictions can be compared to measured data. All of the predictions discussed here include blade-deformation effects and boom-scattering corrections supplied by MRS-BLP. Figure 9 shows a schematic representation of the operating condition parameters used in this study.

Figures 10a–10c show the directivity along the acoustic boom of the first three harmonics, both predicted and data, for all points in the operating condition matrix. Note that positive values of x indicate ahead of the propeller disc in these figures. One clear feature of the results of Fig. 10 is that the trends of the harmonics are well calculated in most conditions. For example, the rapid fall off in sound pressure level aft of the propeller plane is observed in both predictions and data. For the first harmonic, the level of the peak is always overpredicted. The overprediction is generally 2–5 dB except for conditions 360 and 361 where it is about 8 dB. This overprediction is also present at other axial positions. The overprediction at microphone position 1 at almost all flight conditions could likely be due to a microphone malfunction. Evidence of this appears in Table 3, where the measured harmonic levels of the fuselage microphone corresponding to boom microphone 1 are given. The effect of boundary-layer refraction on the propeller noise for this fuselage microphone position should be a reduction in harmonic level. Nevertheless, it is seen that the levels of the first harmonic of this microphone are always

Table 3 Measured results of fuselage microphone corresponding to boom microphone 1

Condition	1 × BPF,[a] dB	2 × BPF, dB	3 × BPF, dB
348	131.4	123.0	115.3
356	134.6	125.3	112.4
357	135.7	127.3	118.3
360	132.2	125.1	118.4
361	133.8	124.5	118.6
377	126.2	118.6	112.1
378	127.8	119.1	—
380	129.2	118.1	—
383	134.1	122.9	113.2

[a]Blade passage frequency

much higher than that measured at boom microphone 1, lending support to the proposed microphone malfunction. The levels measured at boom microphone 5 were most likely affected by reflections from the nacelle and wing leading edge.

For the second and third harmonics, the predicted peak levels are, in general, closer to measured levels. The maximum discrepancy is about 5 dB for the peak values. The directivity shapes are good except for the microphone 5 position and for the lowest rotational tip Mach number of 0.65 at all engine horsepowers. This sudden rise in directivity is unexplained and is perhaps due to nonuniform inflow. The fact that there is now underprediction at microphone 1 supports this suspicion.

Concluding Remarks

In this paper, we have used a series of flight test acoustic data of an advanced propeller to assess the current capability of propeller noise prediction. The best available aeroelastic, aerodynamic, and acoustic codes were employed for this project. Only acoustic data for uniform inflow cases have been used in the study presented here. Direct measurement of inflow parameters was not available, and there are reasons to believe that uniformity of flow into the propeller was only approximated in these tests for a nacelle tilt angle of -1 deg. Some predictions involving nonuniform inflow conditions were calculated as part of the PTA noise-prediction project and are reported elsewhere. An extensive study such as that performed here for the uniform inflow case, however, has not been conducted. It is believed that the main sources of error in our predictions were 1) nonuniform inflow into the propeller; and 2) scattering of sound from the nacelle and wings that was not included in the prediction scheme.

The major conclusions of this study are as follows:

1) Blade deformation can significantly influence propeller aerodynamics and noise. An automated aeroelastic-aerodynamic iteration system has been developed for the inclusion of blade deformation which contains the effects of both centrifugal and blade forces.

2) If the inflow is uniform and the scattering of acoustic waves from noncylindrical geometric objects is negligible, then the current capability for free-field noise prediction for advanced propellers is excellent in trends and generally good in absolute levels.

Future prediction studies should include 1) nonuniform inflow conditions and 2) installation effects and scattering from rigid surfaces near the propeller. For 1, sophisticated unsteady aerodynamics codes are needed. Unfortunately, little experimental data to validate these codes are available. Without full validation of aerodynamic codes, the assessment of noise-prediction technology is not possible. For 2, new methods which model realistic aircraft geometry must be developed. Options, such as the boundary or finite element method, are possible alternatives to classical CFD methods. Appropriate experiments for validation of codes based on such methods must be performed in order to assess their applicability.

Acknowledgments

The authors thank Harold Bartel of Lockheed-Georgia, A. Aljabri of Lockheed-California, Rich August of Sverdrup, Chris Miller of NASA Lewis Research Center, and Bernie Magliozzi and his colleagues at Hamilton Standard for their valuable assistance on various aspects of this project.

References

[1]Little, B. H., Bartel, H. W., Reddy, N. N., Swift, G., Withers, C. C., and Brown, P. C., "Propfan Test Assessment (PTA) Flight Test Report," NASA CR-182278, April 1989.

[2]Little, B. H., Poland, D. T., Bartel, H. W., Withers, C. C., and Brown, P. C., "Propfan Test Assessment (PTA) Final Project Report," NASA CR-185138, July 1989.

[3]Lawrence, C., Aiello, R. A., Ernst, M. A., and McGee, O. G., "A NASTRAN Primer for the Analysis of Rotating Flexible Blades," NASA TM-89861, May 1987.

[4]Aiello, R. A., "Composite Blade Structural Analyzer (COBSTRAN) Users' Manual," NASA TM-101461, April 1989.

[5]Adamczyk, J. J., "Model Equation for Simulating Flows in Multistage Turbomachinery," American Society of Mechanical Engineers, Paper 85-GT-226; also NASA TM-86869, Nov. 1984.

[6]Dunn, M. H., and Tarkenton, G. M., "Computational Methods in the Prediction of Advanced Subsonic and Supersonic Propeller Induced Noise—ASSPIN Users Manual," NASA CR 4434, April 1992.

[7]Spence, P. L., "User's Manual for the Langley Boundary Layer Noise Propagation Program (MRS-BLP)." NASA CR-187559, Aug. 1991.

[8]August, R., and Kaza, K. R. V., "Vibration, Performance, Flutter, and Forced Response Characteristics of a Large-Scale Propfan and Its Aeroelastic Model," AIAA Paper 88-3155, July 1988; also NASA TM-101322, July 1988.

[9]Lawrence, C., and Kielb, R. E., "Nonlinear Displacement Analysis of Advanced Propeller Structures Using NASTRAN," NASA TM-83737, Aug. 1984.

[10]Celestina, M. L., Mulac, R. A., and Adamczyk, J. J., "A Numerical Simulation of the Inviscid Flow Through a Counter-Rotating Propeller," *Transactions of the ASME, Journal of Turbomachinery*, Vol. 108, 1986, pp. 187–193.

[11]Farassat, F., Padula, S. L., and Dunn, M. H., "Advanced Turboprop Noise Prediction Based on Recent Theoretical Results," *Journal of Sound and Vibration*, Vol. 119, No. 1, 1987, pp. 53–79.

[12]Farassat, F., and Succi, G. P., "The Prediction of Helicopter Rotor Discrete Frequency Noise," *Vertica*, Vol. 7, 1983, pp. 309–320.

[13]Farassat, F., "Theoretical Analysis of Linearized Acoustics and Aerodynamics of Advanced Supersonic Propellers," AGARD CP-366 (10), 1985, pp. 1–15.

[14]McAninch, G. L., and Rawls, J. W., "Effects of Boundary Layer Refraction and Fuselage Scattering on Fuselage Surface Noise from Advanced Turboprop Propellers," AIAA Paper 84-0249, Jan. 1984.

[15]Abramowitz, M., and Stegan, I. A., (ed.), *Handbook of Mathematical Functions*, National Bureau of Standards, Washington, DC, 1964 (also published by Dover Books).

[16]Farassat, F., Dunn, M. H., and Spence, P. L., "A Note on Advanced Propeller Noise Prediction in the Time Domain," *AIAA Journal* (to be published).

[17]Block, P. J. W., and Spence, P. L., "Analysis of the PTA External Noise Data," AIAA 13th Aeroacoustics Conf., AIAA Paper 90-3935, Oct. 1990.

[18]Spence, P. L., "Development of a Boundary Layer Noise Propagation Code and its Application to Advanced Propellers," AIAA Paper 91-0593, Jan. 1991; also "Effects of Fuselage Boundary Layer on Noise Prediction from Advanced Propellers," *Journal of Aircraft* (to be published).

[19]Dunn, M. H., and Farassat, F., "State-of-the-Art of High Speed Propeller Noise Prediction—A Multidisciplinary Approach and Comparison with Measured Data," AIAA 13th Aeroacoustics Conf., AIAA Paper 90-3934, Oct. 1990.